

Ultrasensitive and highly selective gas sensors using three-dimensional tungsten oxide nanowire networks

Andrea Ponzoni,^{a)} Elisabetta Comini, and Giorgio Sberveglieri
SENSOR Laboratory, Università di Brescia, Brescia 25121, Italy; CNR-INFM, Università di Brescia, Brescia 25121, Italy; and Dipartimento di Chimica e Fisica, Università di Brescia, Brescia 25121, Italy

Jun Zhou, Shao Zhi Deng, and Ning Sheng Xu^{b)}
School of Physics and Engineering, Sun Yat-Sen (Zhongshan) University, Guangzhou 510275, China; State Key Laboratory, Sun Yat-Sen (Zhongshan) University, Guangzhou 510275, China; and Guangdong Province Key Laboratory of Display Materials and Technologies, Sun Yat-Sen (Zhongshan) University, Guangzhou 510275, China

Yong Ding and Zhong Lin Wang^{c)}
School of Materials Science and Engineering, Georgia Institute of Technology, Atlanta, Georgia 30332-0245

(Received 18 December 2005; accepted 1 March 2006; published online 15 May 2006)

Three-dimensional (3D) tungsten oxide nanowire networks have been demonstrated as a high-surface area material for building ultrasensitive and highly selective gas sensors. Utilizing the 3D hierarchical structure of the networks, high sensitivity has been obtained towards NO₂, revealing the capability of the material to detect concentration as low as 50 ppb (parts per billion). The distinctive selectivity at different working temperatures is observed for various gases. The results highlight that the nanobelts (nanowires) technology can be adopted for the development of gas sensors with performances suitable for practical applications. © 2006 American Institute of Physics. [DOI: 10.1063/1.2203932]

The performance of a solid-state gas sensor is characterized by its sensitivity, stability, and selectivity. The working principle relies on modulation of electrical conductivity due to surface oxidation (reduction) caused by gas exposure. Because only the surface layer is affected by such reactions, the sensitivity is strongly dependent on the surface-to-volume ratio of the material used. This purpose has been pursued by synthesizing layers with a porous morphology to enhance the material surface area. Porosity is enhanced by means of the thick film synthesis approach typically adopted in the gas sensing field. Such high porosity is not easy to achieve by thin film approach. Another approach largely used in the field is the rheotaxial growth and its thermal oxidation (RGTO) method, which allows synthesizing a porous thin film monolayer composed of nanosized grains.^{1,2}

As far as grain size is concerned, it has to be kept in the order of or lower than the debye length, which is the depth into the surface that the chemisorption process can effectively modify the electrical properties of the metal oxide material.³ Although many studies have been presented about this,^{4–6} the primary difficulty still remains in preparation of a sensing material with small crystallite size but stable when operated at higher temperatures for a long period of time. The quality and stability of the small grain size determine the stability of the sensor.

Semiconductor nanowires, nanobelts, and related nanostructures are unique for sensor applications because of their single-crystalline structure, large surface-to-volume ratio, and high stability.⁷ Nanowire based sensors have been demonstrated for detecting gases, proteins, single virus, and

single cancer markers.^{8–10} Nanowires and nanobelts exhibit optimal structural characteristics for both high sensitivity and long-term stability. They may also possess high selectivity by integrating nanowires of different surface characteristics into an array.

In order to demonstrate the performance of the nanobelt (nanowire) based technology, it is necessary to show that it can bring to results at least comparable with the ones reached by means of thick and thin film technologies traditionally adopted in gas sensing field. For example, after 50 years of research, these technologies have demonstrated the capability of WO₃ based gas sensors to detect NO₂ concentration comparable with the outdoor threshold limit (50 ppb) (parts per billion).¹¹

Nanosensors made using nanowires usually have two electrodes that are interconnected by nanowires. The surface-to-volume ratio of the nanowires is an important factor in determining the sensitivity of the sensor. In this letter, gas sensors built using three-dimensional (3D) WO_{3-x} nanowire networks have been shown to be able to detect NO₂ concentration to 50 ppb level. The results highlighted the suitability of the nanobelt/nanowire based sensors for practical applications.

The WO_{3-x} nanowire networks were prepared by thermal evaporation of tungsten powders at ~1400–1450 °C in the presence of oxygen for 10 min. The growth method and growth mechanism of WO_{3-x} nanowire networks had been described in elsewhere.¹² The morphology of the WO_{3-x} nanowire networks was characterized by using scanning electron microscopy (SEM). The SEM images in Fig. 1 clearly demonstrate the shape of the 3D nanowire networks and the huge surface area, making it more suited for gas sensing application. The network is composed by nanowires with widths ranging from several tens of nanometers to

^{a)}Electronic mail: andrea.ponzoni@ing.unibs.it

^{b)}Electronic mail: stsxns@zsu.edu.cn

^{c)}Electronic mail: zhong.wang@gatech.edu

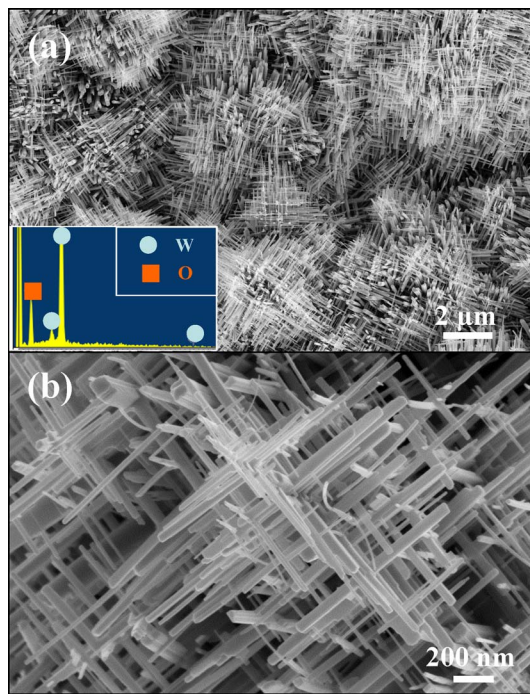


FIG. 1. (Color online) Low magnification (a) and high magnification (b) SEM images of tungsten oxide nanowire network. Inset in (a) is the EDS of the tungsten oxide nanowire networks.

200 nm and the nanowires intercross with each other to form the 3D networks. In particular, each network is about 1–10 μm large and extends its arms along all the three directions (a single nanobelt will instead extend only in the horizontal plane) thus strongly enhances the scattering probability with gaseous molecules and behaving like a porous thick film. An energy dispersive x-ray spectroscopy (EDS) analysis [inset in Fig. 1(a)] indicates that the networks are dominated by W and O elements. Figure 2(a) shows a typical TEM image of a broken WO_{3-x} nanowire network segment with several junctions. The inset of Fig. 2(a) is the corresponding dark field transmission electron microscopy (TEM) image which reveals that there are many defects in the nanowire network. Corresponding selected area electron diffrac-

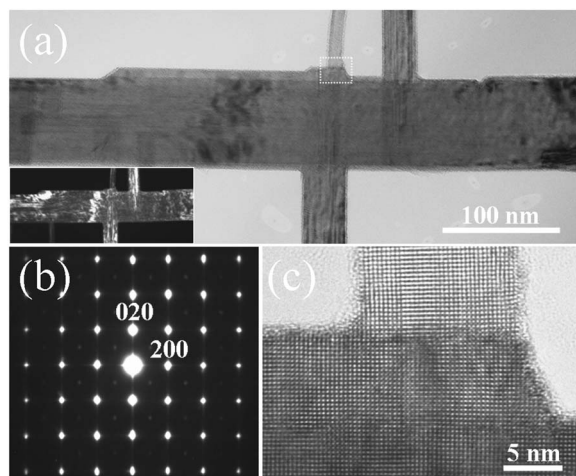


FIG. 2. (a) TEM image of a broken WO_{3-x} nanowire network segment with several junctions. Inset: Dark field TEM image. (b) Corresponding selected area electron diffraction (SAED) pattern of (a). (c) High resolution TEM image taken from the rectangle-closed area in (a).

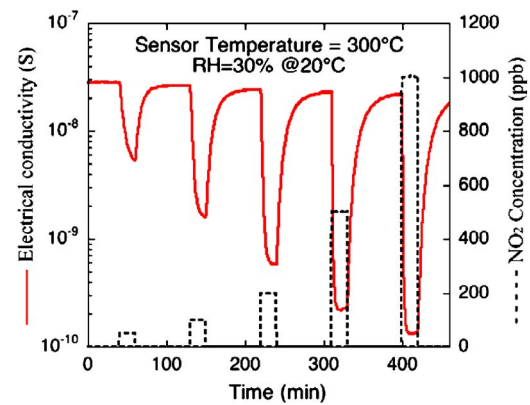


FIG. 3. (Color online) Sensor response to NO_2 of different concentrations, measured at 300 $^{\circ}\text{C}$ and 30% of relative humidity (at 20 $^{\circ}\text{C}$).

tion (SAED) patterns [Fig. 2(b)] were recorded proving that the whole network is single crystalline. The streaks in the SAED patterns were caused by the planar defects along the growth direction of the nanowires.¹² Figure 2(c) is a high resolution TEM image that taken from the rectangle-closed area in Fig. 2(a). The network is formed by switching the growth directions among $\langle 100 \rangle$, thus, each network is a single crystal without internal grain boundaries. We believe that the presence of the ordered-in plane oxygen vacancies in $\{100\}$ planes is the driving mechanism for the formation of 3D network.¹² So far, the sensitivity is expected to be higher than the one reached by either nanowires or nanobelts.

Sensors have been fabricated by drop coating of WO_{3-x} nanowire networks onto a $2 \times 2 \times 0.25 \text{ mm}^3$ alumina substrates provided with interdigitated Pt contacts (200 μm large and separated by 200 μm) built on the front side. A Pt meander had been deposited on the back side, which acts as heating element and temperature probe. Gas sensing measurements have been carried out in a thermostatic chamber with the flowthrough method. Atmosphere composition was controlled by certified bottles of synthetic air containing controlled amount of target gases and a humidifier system. dc electrical conductivity of the sensitive layer has been monitored applying a 1 V voltage and measuring the electrical current by means of a picoammeter.

Gas sensing capability of the material has been measured towards oxidizing (NO_2) and reducing gases (H_2S , CO, and NH_3). Due to the high content of oxygen vacancies, the above samples have been annealed in air at 300 $^{\circ}\text{C}$ for six days with the aim of achieving stoichiometry and stabilizing the electrical properties of the material. The material revealed highly performing towards NO_2 . Responses measured towards a wide range of NO_2 concentrations heating the device at 300 $^{\circ}\text{C}$ are reported in Fig. 3. The results demonstrate the capability of the material to detect up to 50 ppb of NO_2 with the electrical resistance increasing of about six times. A comparison with literature highlights the high sensitivity of the device. For example, one of the best performing WO_3 based sensor has been developed by Wang *et al.*, which report a response $\Delta G/G_0$ of about 1 towards 50 ppb of NO_2 .¹¹

Responses exhibited by both as deposited and annealed samples towards 10 ppm of H_2S are presented in Fig. 4. The results are representative of sensitivity improvements for over 20 times as a result of annealing treatment in reducing gases. Temperature influence on sensing performances has been studied in the 100–500 $^{\circ}\text{C}$ range. The results are sum-

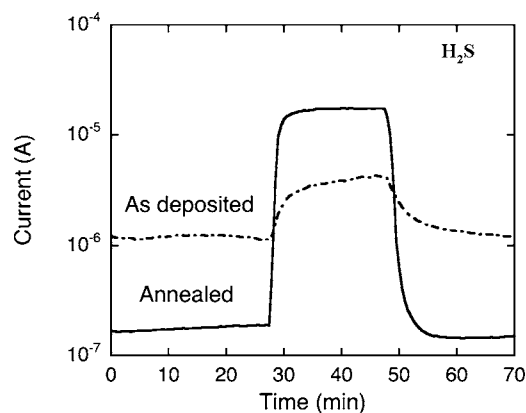


FIG. 4. Sensor response to 10 ppm of H_2S gas, measured at 300°C and with 30% of relative humidity (at 20°C).

marized in Fig. 5. Response has been calculated as $\Delta G/G_0$ for reducing gases and as $\Delta R/R_0$ for oxidizing ones, according to the usually adopted convention for n -type metal oxides. ΔG and ΔR are the electrical conductance and resistance changes caused by gas injection, while G_0 and R_0 are the conductance and resistance values before gas injection. Focusing on NO_2 , it can be observed that response intensity is enhanced by decreasing the sensor temperature to 100°C , but at the same time, decreasing the working temperature slows down the kinetic of the gas-surface reaction so that sensing performances becomes affected by long response and recovery time. For example, working at 200°C , the sensor needs more than 40 min to fully recover its base line signal after NO_2 exposure. So far, 300°C appears the best temperature to achieve performances optimization, in terms of both response intensity and dynamics. Also, for H_2S gas, the response intensity is enhanced when the sensor temperature was increased to 250°C , when the sensor temperature was higher than 350°C the device exhibits weak responses towards the working temperature.

As far as CO and NH_3 are concerned, the device exhibits weak responses towards both gases at any working temperature, which weakly affects response intensities (see Fig. 4). From an applicative point of view, the temperature influence on sensing performances with different gases is a promising feature for the development of a NO_2 sensor with low cross sensitivity towards possible interfering gases.

It is worth to note that the preparation technique and material microstructure can strongly modify gas sensing per-

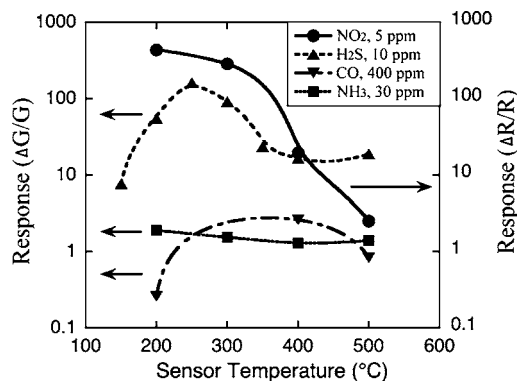


FIG. 5. Sensor response to NO_2 , H_2S , NH_3 , and CO as a function of working temperature. Relative humidity is 30% at the chamber temperature of 20°C .

formances of a given metal oxide. Indeed, the low sensitivity of WO_3 to NH_3 is not a uniqueness of WO_3 but it is related to particular features that have not yet fully addressed. As an example, it has been reported in literature both on WO_3 layers highly sensitive towards ammonia¹³ and WO_3 layers weakly sensitive towards ammonia.¹⁴ Comparing these findings with the present results, it can be observed that three-dimensional nanowire networks exhibit at the same time higher response towards NO_2 and weaker response towards NH_3 .

In summary, the present work has been addressed to study gas sensing performances of three-dimensional WO_{3-x} nanowire networks, which appeared as a promising material for such an application due to its unique microstructure. The results highlighted that this material can be applied in gas sensing field to develop NO_2 sensors with performances suitable for practical application. In particular, the capability to reveal NO_2 concentrations comparable with the threshold limit of outdoor application has been observed, together with low cross sensitivity towards possible interfering gases such as H_2S , NH_3 , and CO . The outdoor application, due to its low threshold limit, is considered as the frontier also for thin and thick film technology typically adopted in gas sensing field. The present results thus demonstrate that nanobelt (nanowire) technology can be used to reach results at least comparable with the best ones obtained by the “traditional” technology.

Three of the authors (A.P., E.C., and G.S.) thank for the financial support of the European Strep project NANOS4 (Grant No. 001528). Two of the authors (S.Z.D. and N.S.X.) thank the support of the project from the NSFC, the Ministry of Science and Technology of China, the Education Ministry of China, the Department of Education and Department of Science and Technology of Guangdong Province, and Department of Science and Technology of Guangzhou City. Another author (Z.L.W.) thanks the support from NSF, the NASA Vehicle Systems, Department of Defense Research and Engineering (DDRE), and the Defense Advanced Research Projects Agency (Award No. N66001-04-1-8903). One of the authors (J.Z.) is thankful for the Kaisi Fund from Sun Yat-sen University.

¹G. Sberveglieri, G. Faglia, S. Groppelli, and P. Nelli, *Semicond. Sci. Technol.* **5**, 1231 (1990).

²N. Barsan, M. Schweizer-Berberich, W. Gopel, and W. Frensenius, *J. Anal. Chem. USSR* **365**, 287 (1999).

³S. R. Morrison, *The Chemical Physics of Surfaces* (Plenum, New York, 1997).

⁴N. Yamazoe, *Sens. Actuators B* **5**, 7 (1991).

⁵A. Rothschild and Y. Komem, *J. Appl. Phys.* **95**, 6374 (2004).

⁶N. Barsan and U. Weimar, *J. Electroceram.* **7**, 143 (2001).

⁷E. Comini, G. Faglia, G. Sberveglieri, Z. W. Pan, and Z. L. Wang, *Appl. Phys. Lett.* **81**, 1869 (2002).

⁸M. Curreli, C. Li, Y. H. Sun, B. Lei, M. A. Gunderson, M. E. Thomson, and C. W. Zhou, *J. Am. Chem. Soc.* **127**, 6922 (2005).

⁹F. Patolsky, G. F. Zheng, O. Hayden, M. Lakadamyali, X. W. Zhuang, and C. M. Lieber, *Proc. Natl. Acad. Sci. U.S.A.* **101**, 14017 (2004).

¹⁰G. F. Zheng, F. Patolsky, Y. Cui, W. U. Wang, and C. M. Lieber, *Nat. Biotechnol.* **23**, 1294 (2005).

¹¹S. H. Wang, T. C. Chou, and C. C. Liu, *Sens. Actuators B* **94**, 343 (2003).

¹²J. Zhou, Y. Ding, S. Z. Deng, L. Gong, N. S. Xu, and Z. L. Wang, *Adv. Mater. (Weinheim, Ger.)* **17**, 2107 (2005).

¹³H. Meixner, J. Gerblinger, U. Lampe, and M. Fleischer, *Sens. Actuators B* **23**, 119 (1995).

¹⁴A. Ponzoni, E. Comini, M. Ferroni, and G. Sberveglieri, *Thin Solid Films* **490**, 81 (2005).